

Ras-mediated activation of the TORC2–PKB pathway is critical for chemotaxis

Huaqing Cai,¹ Satarupa Das,² Yoichiro Kamimura,¹ Yu Long,¹ Carole A. Parent,² and Peter N. Devreotes¹

¹Department of Cell Biology, Johns Hopkins University, School of Medicine, Baltimore, MD 21205

²Laboratory of Cellular and Molecular Biology, Center for Cancer Research, National Cancer Institute, National Institutes of Health, Bethesda, MD 20892

In chemotactic cells, G protein–coupled receptors activate Ras proteins, but it is unclear how Ras-associated pathways link extracellular signaling to cell migration. We show that, in *Dictyostelium discoideum*, activated forms of RasC prolong the time course of TORC2 (target of rapamycin [Tor] complex 2)–mediated activation of a myristoylated protein kinase B (PKB; PKBR1) and the phosphorylation of PKB substrates, independently of phosphatidylinositol-(3,4,5)-trisphosphate. Paralleling these changes, the kinetics of chemoattractant-induced adenylyl cyclase activation and actin polymerization are extended, pseudopodial activity is increased and mislocalized, and

chemotaxis is impaired. The effects of activated RasC are suppressed by deletion of the TORC2 subunit PiaA. In vitro RasC^{G62L}–dependent PKB phosphorylation can be rapidly initiated by the addition of a PiaA-associated immunocomplex to membranes of TORC2-deficient cells and blocked by TOR-specific inhibitor PP242. Furthermore, TORC2 binds specifically to the activated form of RasC. These results demonstrate that RasC is an upstream regulator of TORC2 and that the TORC2–PKB signaling mediates effects of activated Ras proteins on the cytoskeleton and cell migration.

Introduction

Chemotaxis, the capacity of cells to migrate directionally in response to gradients of extracellular chemical cues, plays an important role in many biological processes, including embryogenesis, neuronal patterning, wound healing, and immune cell trafficking. Conversely, improper chemotaxis underlies various pathological conditions, including many chronic inflammatory diseases. Altered cell motility is a hallmark of transformed cells, and chemotactic homing assists in the migration of cancer cells from primary tumors to metastatic sites.

Studies of the model organism *Dictyostelium discoideum* have greatly contributed to our understanding of eukaryotic chemotaxis. In *D. discoideum*, chemoattractant gradients detected by G protein–coupled receptors are converted into localized intracellular signals to direct cell migration (Franca-Koh et al., 2006; Iglesias and Devreotes, 2008; King and Insall, 2009). For example, phosphatidylinositol-(3,4,5)-trisphosphate (PIP3) at the leading edge of chemotaxing cells promotes cytoskeleton

rearrangements possibly by recruiting pleckstrin homology (PH) domain–containing proteins such as PKB A (PKBA; Parent et al., 1998; Meili et al., 1999). We have recently described a circuit involving TORC2 (target of rapamycin [Tor] complex 2) and its substrate PKBR1 that functions in parallel with the PIP3 pathway to regulate chemotaxis (Kamimura et al., 2008). Unlike PKBA, PKBR1 is tethered to the plasma membrane via the N-terminal myristoylation (Meili et al., 2000). With uniform chemoattractant stimulation, both PKBA and PKBR1 are transiently phosphorylated within their hydrophobic motifs (HMs) via TORC2 and subsequently phosphorylated within their activation loops (ALs) by phosphoinositide-dependent kinases (PDKs; Fig. 1 A; Kamimura et al., 2008; Kamimura and Devreotes, 2010). The HM phosphorylation is essential for the activation of PKBR1 and also contributes to the activation of PKBA. In migrating cells, these phosphorylation events are restricted to the cell's leading edge (Kamimura et al., 2008).

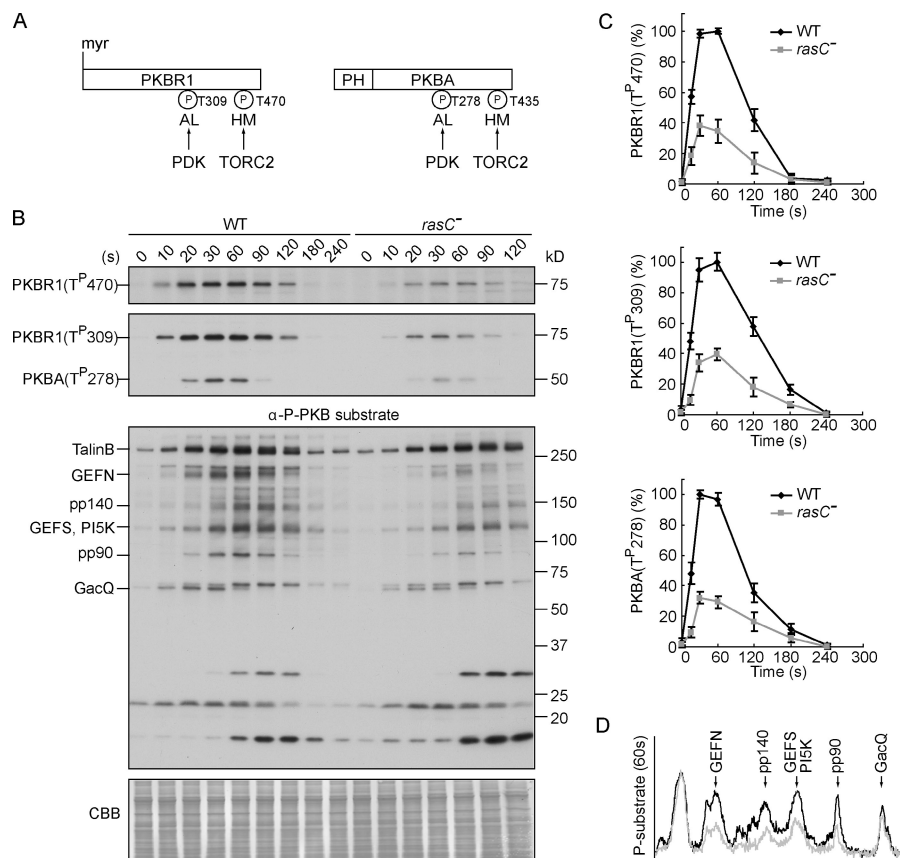
Correspondence to Peter N. Devreotes: pnd@jhmi.edu

Abbreviations used in this paper: ACA, adenylyl cyclase; AL, activation loop; DB, development buffer; HM, hydrophobic motif; HSS, high-speed supernatant; PDK, phosphoinositide-dependent kinase; PH, pleckstrin homology; PI3K, phosphoinositide 3-kinase; PIP3, phosphatidylinositol-(3,4,5)-trisphosphate; RBD, Ras-binding domain; Tor, target of rapamycin.

© 2010 Cai et al. This article is distributed under the terms of an Attribution–Noncommercial–Share Alike–No Mirror Sites license for the first six months after the publication date (see <http://www.rupress.org/terms>). After six months it is available under a Creative Commons license (Attribution–Noncommercial–Share Alike 3.0 Unported license, as described at <http://creativecommons.org/licenses/by-nc-sa/3.0/>).

Figure 1. RasC is required for the activation of the PKB pathway. (A) Schematic representation of the activation of PKBR1 and PKBA.

PKBR1 is tethered to the plasma membrane via myristoylation, whereas PKBA is recruited to the plasma membrane by PIP3 via the PH domain. Upon chemoattractant stimulation, the two PKBs are activated through phosphorylation of their HMs by TORC2 and ALs by PDK. (B) Wild-type (WT) or *rasC*[−] cells were stimulated with cAMP, sampled at the indicated time points, and probed with anti-phospho-HM (first panel), anti-phospho-AL (second panel), or anti-phospho-substrate antibodies (third panel). The protein-transferred membrane was stained with Coomassie brilliant blue (CBB) and shown as loading control (fourth panel). Seven proteins, including TalinB, GEFN, GEFS, PI5K, and GacQ, are confirmed PKB substrates. Note that TalinB co-migrates with a non-PKB substrate band, and unmarked bands at the bottom part of the third panel are not PKB substrates (Kamimura et al., 2008). (C) Quantitative densitometry of the first and second panels of B, showing the mean intensity \pm SD of the respective bands from three independent experiments. (D) Densitometric scan of the 60-s lanes of the third panel of B (wild type, black line; *rasC*[−], gray line).



These observations suggest that the activity of TORC2 is both temporally and spatially regulated in chemotactic cells, and similarly, the catalytic activity of mammalian TORC2 is reported to be stimulated by growth factors (Sarbasov et al., 2005; Frias et al., 2006; Huang et al., 2008). Although the TORC2 regulators are unidentified, several lines of evidence have suggested that the Ras family small GTPases may play a role. Ras proteins are activated by chemoattractant in *D. discoideum* with time courses that parallel TORC2 activation (Kae et al., 2004; Zhang et al., 2008). The *D. discoideum* TORC2 subunit Rip3 and its yeast and mammalian homologues all contain a putative Ras-binding domain (RBD). Rip3 interacts with the GTP-bound form of *D. discoideum* RasG and human H-Ras in yeast two-hybrid assays (Lee et al., 1999, 2005). In a cell-free system that we previously developed, GTP- γ S is able to trigger TORC2-mediated activation of PKBR1 (Kamimura et al., 2008). Though suggestive, these observations do not prove that Ras proteins directly regulate TORC2, and indeed, there are several inconsistencies. For example, disruption of RasG has little or no effect on PKB phosphorylation or chemotaxis (Sasaki et al., 2004; Kamimura et al., 2008).

In this study, we use a combination of genetic interaction strategies and in vitro reconstitution assays to determine whether Ras family proteins activate TORC2 and to examine the effects of this putative pathway on directed cell migration and chemotactic responsiveness. We report that a specific Ras protein, RasC, activates TORC2 and exerts temporal and spatial control on the TORC2-PKBR1 pathway to regulate chemotaxis.

Results

RasC is required for TORC2-mediated activation of PKB

Pursuing our earlier observation suggesting that Ras proteins may regulate the two PKBs (Kamimura et al., 2008), we examined PKB activity in cells in which different Ras genes were disrupted. In wild-type cells, cAMP triggered rapid phosphorylation of the HM of PKBR1 and the ALs of PKBR1 and PKBA, which peaked at 30–60 s and declined to the prestimulus level by 2–3 min (Fig. 1 B). Consequently, a series of PKB substrates were also transiently phosphorylated (Fig. 1 B). We previously found that these phosphorylations were reduced in *rasC*[−]/*rasG*[−] but not in *rasG*[−] cells, suggesting that either RasC or both Ras proteins are needed (Fig. S1 A; Kamimura et al., 2008). In this study, we show that, compared with wild-type cells, phosphorylations of the HM of PKBR1 and the ALs of PKBR1 and PKBA were reduced by 60–70% by deleting RasC alone (Fig. 1, B and C; and Fig. S1 B). There was also a significant reduction in the phosphorylation of many PKB substrates (Fig. 1 D). Expression of Flag-tagged RasC in *rasC*[−] cells restored all of these phosphorylation events (data described in the next paragraph). These results suggest that RasC is a regulator of the PKB pathway. However, because of the residual phosphorylation of the PKBs and PKB substrates present in *rasC*[−] cells, which may be due to the presence of other chemoattractant-activated Ras proteins (Fig. S1 C), and the fact that *rasC*[−] cells display better chemotaxis compared with cells lacking the two PKBs (Meili

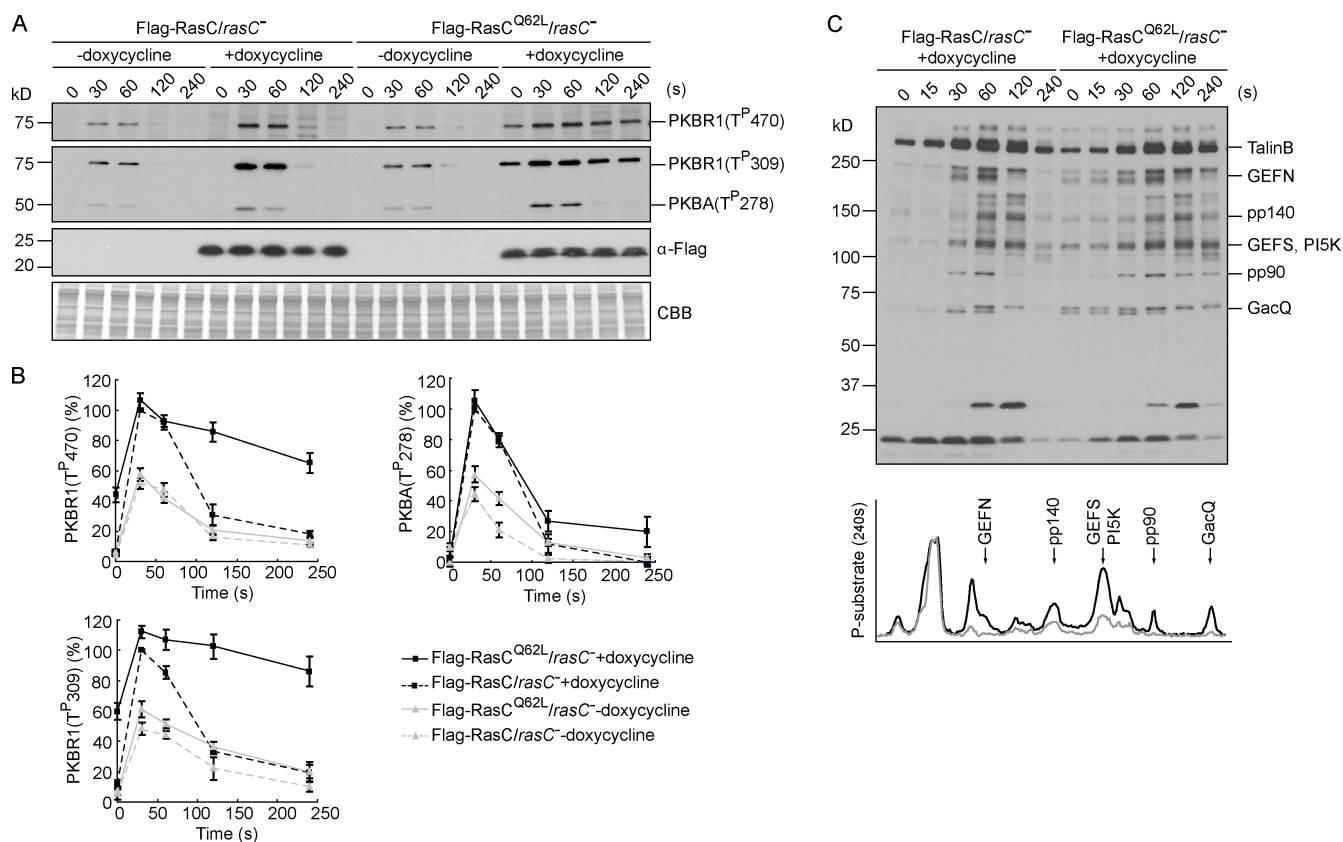


Figure 2. Persistently activated RasC alters the time course of PKBR1 and PKB substrate phosphorylation. (A) Flag-RasC or -RasC^{Q62L} was expressed under the control of a doxycycline-inducible promoter in *rasC*⁻ cells. Cells developed in the presence or absence of doxycycline were stimulated with cAMP, sampled at the indicated time points, and probed with phospho-specific antibodies or anti-Flag antibody. The protein-transferred membrane was stained with Coomassie brilliant blue (CBB) and shown as loading control. (B) Quantitative densitometry of the first and second panels of A, showing the mean intensity \pm SD of the respective bands from four independent experiments. (C) Samples were probed with anti-phospho-substrate antibody (top). Densitometric scans of the 240-s lanes are shown in bottom panel (Flag-RasC, gray line; Flag-RasC^{Q62L}, black line).

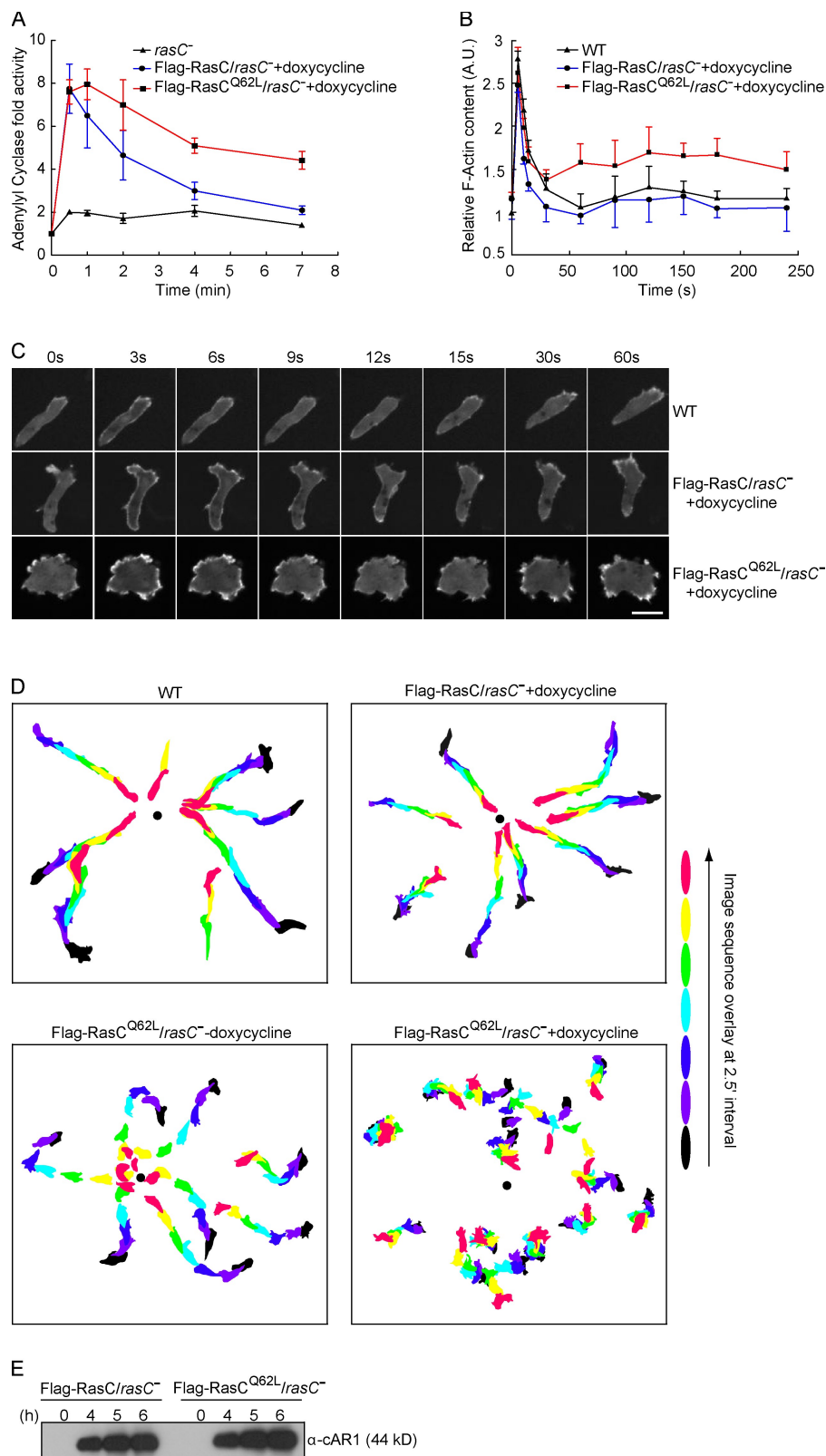
et al., 1999, 2000; Lim et al., 2001; Kamimura et al., 2008), further evidence is needed to prove this hypothesis.

We reasoned that if RasC indeed regulates the PKB pathway, the kinetics of PKB phosphorylation might be changed by altering the lifetime of RasC activation. To assess this possibility, we expressed Flag-tagged wild-type or activated form of RasC (RasC^{Q62L}) in *rasC*⁻ cells under the control of a doxycycline-inducible promoter. An equivalent mutation (Q61L) in human H-Ras was reported to have both increased nucleotide exchange and decreased GTPase activity (Feig and Cooper, 1988), and indeed, we found RasC^{Q62L} to be persistently activated (unpublished data). The expression of Flag-RasC or -RasC^{Q62L} was not detectable before doxycycline induction (Fig. 2 A). Consequently, the Flag-RasC/*rasC*⁻ and -RasC^{Q62L}/*rasC*⁻ cells exhibited reduced PKB phosphorylation similar to *rasC*⁻ cells (compare Fig. 2 [A and B] with Fig. 1 [B and C]). 2–3 h after induction, the levels of Flag-RasC and -RasC^{Q62L} reached 3.9 ± 0.9 - and 2.6 ± 0.4 -fold of the level of endogenous RasC in wild-type cells (Fig. 2 A and not depicted). The expression of Flag-RasC restored the phosphorylation of PKBR1 and PKBA to near wild-type patterns (compare Fig. 2 [A and B] with Fig. 1 [B and C]). The expression of Flag-RasC^{Q62L} also restored the phosphorylation events, but for the HM and AL of PKBR1, it elevated the basal level and greatly

extended the kinetics (Fig. 2, A and B). The half-life of HM phosphorylation of PKBR1 was ~ 40 s in cells expressing Flag-RasC but was extended to ~ 140 s in cells expressing Flag-RasC^{Q62L}. The half-life of AL phosphorylation of PKBR1 was similarly prolonged. In contrast, AL phosphorylation of PKBA was negligibly changed in the presence of Flag-RasC^{Q62L}, although the profile sometimes remained slightly elevated at later time points (Fig. 2, A and B). Consistent with our previous finding that PKBR1 provides the primary PKB activity (Kamimura et al., 2008), many PKB substrates remained in their phosphorylated state at later time points in Flag-RasC^{Q62L}-expressing cells (Fig. 2 C). Similar results were obtained when Flag-RasC or -RasC^{Q62L} was expressed in *rasC*⁻ cells using a noninducible promoter (Fig. S2, A–C). We also found that the expression of Flag-tagged RasC^{G13V}, another activated form of RasC, modestly lengthened the activation of PKBR1 (Fig. S2 D). The extended kinetics of PKBR1 phosphorylation correlated with the slow turn-off of RasC caused by Q62L and G13V mutations, indicating that the transient activation of RasC sets the time course of the PKB pathway. In contrast, the expression of activated form of RasG (RasG^{Q61L}) did not affect PKB phosphorylation (Fig. S1 D), again suggesting a specific role for RasC in regulating the PKB pathway.

Figure 3. Chemotactic responses are altered in cells with prolonged PKBR1 signaling.

(A) ACA activation upon uniform cAMP stimulation was measured in *rasC⁻* cells or *rasC⁻* cells induced to express Flag-RasC or -RasC^{Q62L}. The data represent the range (mean \pm standard error) of two independent experiments. The basal activities ranged from 1.9 pmol/min/mg protein for *rasC⁻* to 2.5 pmol/min/mg protein for Flag-RasC/*rasC⁻* and 3.8 pmol/min/mg protein for Flag-RasC^{Q62L}/*rasC⁻* cells. (B) Actin polymerization was measured in wild-type (WT) cells or *rasC⁻* cells expressing Flag-RasC or -RasC^{Q62L}. Cells were stimulated with cAMP and lysed with Triton X-100 buffer. The Triton-insoluble pellet fraction was analyzed by SDS-PAGE and Coomassie blue staining. The amount of actin in the pellet was quantified by densitometry. The data represent mean \pm SD of three independent experiments. A.U., arbitrary unit. (C) The translocation of LimE Δ coil-RFP was recorded by fluorescence microscopy with images taken every 3 s. Frames from the indicated time points after the addition of cAMP are shown. (D) The chemotactic movements to a micropipette releasing 1 μ M cAMP (black dot) were recorded by time-lapse microscopy. Images from frames at 2.5-min intervals were processed to outline the cells, color coded for each time point, and overlaid. (E) The expression of cAR1 is comparable in *rasC⁻* cells induced to express Flag-RasC or -RasC^{Q62L}. At the indicated time points after initiation of development, CHAPS-insoluble membrane fractions were prepared as described previously (Xiao et al., 1997) and probed with anti-cAR1 antibody. Bar, 10 μ m.



Proper temporal and spatial regulation of the PKBR1 pathway is critical for chemotaxis

To assess the effect of prolonged activation of RasC and PKB signaling, we analyzed a series of chemotactic responses as

well as chemotaxis in *rasC⁻* cells induced to express Flag-RasC or -RasC^{Q62L}. We first measured the cells' capacity to activate adenylyl cyclase (ACA) in response to chemoattractant stimulation because RasC (Lim et al., 2001), TORC2 (Chen et al., 1997; Lee et al., 2005), and the two PKBs (Fig. S3)

Table I. Quantification of cellular behavior

Strain	Motility speed	Chemotax motility	Chemotax index	Persistency
	$\mu\text{m}/\text{min}$	$\mu\text{m}/\text{min}$		
Wild type	7.13 ± 0.53	6.04 ± 1.07	0.81 ± 0.09	0.87 ± 0.08
Flag-RasC/ <i>rasC</i> [−] + doxycycline	7.75 ± 1.39	6.30 ± 1.22	0.79 ± 0.05	0.83 ± 0.01
Flag-RasC ^{Q62L} / <i>rasC</i> [−] − doxycycline	6.55 ± 0.98	5.20 ± 0.91	0.69 ± 0.02	0.79 ± 0.05
Flag-RasC ^{Q62L} / <i>rasC</i> [−] + doxycycline	5.10 ± 1.78	1.06 ± 0.52	0.09 ± 0.25	0.31 ± 0.15
Flag-RasC/ <i>aca</i> [−] + doxycycline	4.62 ± 0.47	3.94 ± 0.53	0.82 ± 0.07	0.84 ± 0.06
Flag-RasC ^{Q62L} / <i>aca</i> [−] + doxycycline	3.94 ± 0.49	0.77 ± 0.24	0.14 ± 0.14	0.46 ± 0.04
Flag-RasC/ <i>piaA</i> [−] + doxycycline	5.68 ± 1.14	2.92 ± 0.71	0.46 ± 0.03	0.60 ± 0.08
Flag-RasC ^{Q62L} / <i>piaA</i> [−] + doxycycline	5.24 ± 0.37	2.79 ± 0.16	0.44 ± 0.07	0.56 ± 0.01
Flag-RasC ^{Q62L} / <i>piaA</i> [−] − doxycycline	5.59 ± 0.65	3.04 ± 0.45	0.53 ± 0.04	0.62 ± 0.04

Quantitation of the chemotactic behavior of at least 10 cells from at least three independent experiments. Motility and chemotactic parameters are calculated as described in Materials and methods. The data represent mean \pm SD.

are all required for the activation of the enzyme. Similar to wild-type cells, the Flag-RasC-expressing cells displayed a rapid rise in ACA activity, peaking at 30 s after the addition of cAMP, followed by a return to the prestimulus level with a half-time of ~ 1.8 min (Fig. 3 A). In contrast, the half-time of decline was prolonged to ~ 5 min in cells expressing Flag-RasC^{Q62L} (Fig. 3 A). As a control, in the absence doxycycline, the Flag-RasC/*rasC*[−] and -RasC^{Q62L}/*rasC*[−] cells showed greatly reduced ACA activation (not depicted) similar to *rasC*[−] cells (Fig. 3 A).

We next monitored chemoattractant-induced changes in actin polymerization and the distribution of the actin-binding protein LimEΔcoil, which labels newly formed F-actin (Schneider et al., 2003). In wild-type cells and *rasC*[−] cells expressing Flag-RasC, uniform exposure to chemoattractant triggered two phases of actin polymerization (Fig. 3 B). An initial large peak occurred within a few seconds, followed by a rapid decrease and a subsequent lower peak centered around 2 min. Paralleling these changes, LimEΔcoil-RFP first translocated uniformly to the cell cortex, then returned to the cytosol as cells rounded up, and finally localized to regions of newly formed pseudopods during the second phase (Fig. 3 C and Video 1). Compared with these two cell lines, cells expressing Flag-RasC^{Q62L} exhibited elevated F-actin polymerization, especially in the second phase (Fig. 3 B). When observed under the microscope, the cells were less polarized and displayed an increased number of F-actin-rich membrane protrusions (Fig. 3 C and Video 2).

We then compared the chemotactic behavior of wild-type cells and cells expressing Flag-RasC or -RasC^{Q62L} (Fig. 3 D and Table I). When placed in chemoattractant gradients generated by a micropipette releasing cAMP, wild-type cells rapidly polarized and migrated toward the higher concentrations with a focused leading edge (Video 3). Without doxycycline, the chemotactic responses of Flag-RasC/*rasC*[−] (not depicted) and -RasC^{Q62L}/*rasC*[−] cells were slightly affected compared with wild-type cells (Video 4). After induction with doxycycline, Flag-RasC-expressing cells migrated robustly toward the micropipette with motility and chemotactic parameters equivalent to wild-type cells (Video 5). In contrast, cells expressing Flag-RasC^{Q62L} showed reduced directionality to the chemoattractant source. They displayed selective defects in chemotactic index, chemotactic motility, and persistency compared with the other cell lines (Video 6). The chemotaxis defect in these cells was not

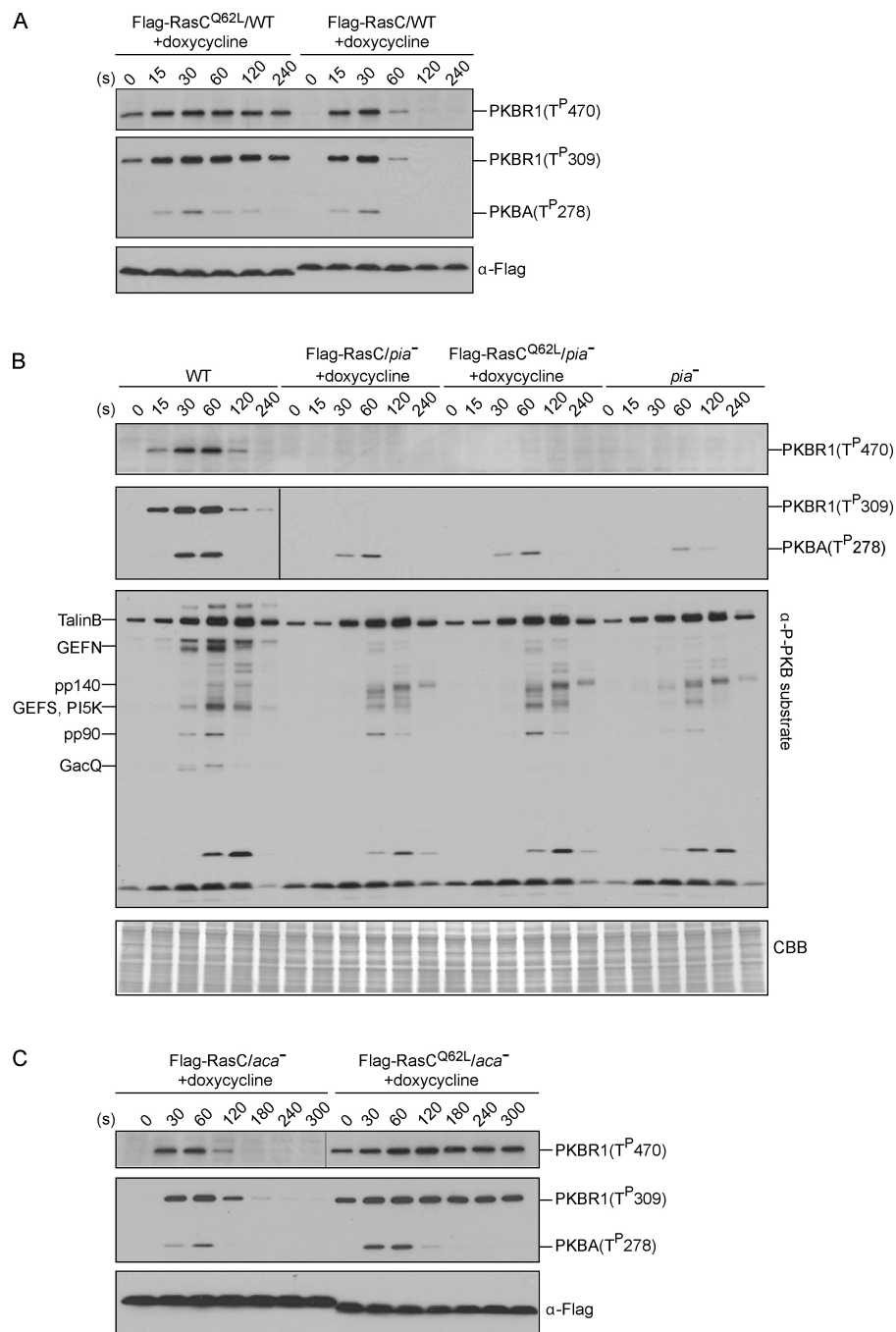
caused by a delay in cell differentiation, as the expression of the cAMP receptor, cAR1, was not impacted (Fig. 3 E). A chemotaxis defect was also observed when Flag-RasC^{Q62L} was expressed in the *rasC*[−] cells using a noninducible promoter (Fig. S2, E and F), although cAR1 expression was partially impaired in these cells (not depicted). Collectively, these results imply that the failure to temporally control PKBR1 activation alters the chemotactic responsiveness of cells expressing RasC^{Q62L} and prevents them from performing directional migration efficiently.

The effects of activated RasC on chemotactic responses and chemotaxis are suppressed in *piaA*[−] cells

If the aberrant chemotactic behavior displayed in RasC^{Q62L}-expressing cells results from the unregulated PKBR1 activity, these responses should be suppressed in cells in which the prolonged PKBR1 activation is blocked. To test this, we expressed Flag-RasC or -RasC^{Q62L} in cells lacking the essential TORC2 component PiaA and compared the chemotactic responses of these cells with wild-type controls. Deletion of PiaA did not impair the activation of RasC (Fig. S4). Wild-type cells induced to express Flag-RasC^{Q62L} exhibited prolonged phosphorylation of PKBR1 (Fig. 4 A). In contrast, in *piaA*[−] or *piaA*[−] cells induced to express Flag-RasC or -RasC^{Q62L}, chemoattractant-triggered phosphorylation of PKBR1 was abolished, and phosphorylations of PKBA and PKB substrates were reduced (Fig. 4 B). Consistent with our hypothesis, deletion of PiaA prevented the extended ACA activation and actin polymerization responses observed in wild-type controls expressing Flag-RasC^{Q62L} (Fig. 5, A and B).

We then performed the micropipette assay on these cells. Because ACA activity was dramatically reduced in *piaA*[−] cells (Fig. 5 A), we chose *aca*[−] cells, which have been reported to display robust chemotaxis (Kriebel et al., 2003), as controls. Similar to *rasC*[−] cells, expressing Flag-RasC^{Q62L} in *aca*[−] cells disrupted the normal transient kinetics of phosphorylation of PKBR1 (Fig. 4 C), and the cells displayed greatly reduced chemotaxis compared with *aca*[−] cells expressing Flag-RasC (Fig. 5 C, Table I, and Videos 7 and 8). This result incidentally shows that the deleterious effects of RasC^{Q62L} on chemotaxis are not mediated through elevated cAMP. Deletion of PiaA suppressed the chemotaxis defects caused by RasC^{Q62L}. Although partially

Figure 4. Deletion of the TORC2 component *PiaA* suppresses the prolonged phosphorylation of PKBR1 and PKB substrates caused by *RasC^{Q62L}*. (A–C) Flag-RasC or -RasC^{Q62L} was expressed under the control of a doxycycline-inducible promoter in wild-type (WT; A), *piaA*[−] (B), or *aca*[−] cells (C). Cells were stimulated with cAMP, sampled at the indicated time points, and probed with phospho-specific antibodies or anti-Flag antibody. The protein-transferred membrane was stained with Coomassie brilliant blue (CBB) and shown as loading control. Vertical black lines indicate that intervening lanes have been spliced out.



impaired, *piaA*[−] cells expressing Flag-RasC^{Q62L} showed comparable motility and chemotactic parameters compared with *piaA*[−] cells expressing Flag-RasC (Fig. 5 C, Table I, and Videos 9 and 10). These results present a strong genetic link between RasC and TORC2 and imply that RasC acts through TORC2 to control PKBR1 and chemotaxis.

PIP3 is not required for RasC-mediated activation of PKBR1

In many systems, phosphoinositide 3-kinases (PI3Ks) are effectors of Ras proteins, and PIP3 recruits Akt/PKB to the plasma membrane and facilitates its activation (Cantley, 2002; Karnoub and Weinberg, 2008). However, only PKBA, but not

PKBR1, contains a PIP3-responsive PH domain. Therefore, we investigated whether the prolonged activation of PKBR1 in Flag-RasC^{Q62L}-expressing cells depends on PI3K. As shown in Fig. 6 A, the time course of PIP3 production upon chemoattractant stimulation was essentially identical in cells expressing Flag-RasC or -RasC^{Q62L}, indicating that RasC^{Q62L} does not activate PI3K. Next, we expressed Flag-RasC or -RasC^{Q62L} in *pi3k1*^{−/2} cells. Because these cells contain no detectable PIP3 (Huang et al., 2003), AL phosphorylation of PKBA was completely abolished (Fig. 6 B). In contrast, Flag-RasC^{Q62L} increased the basal level and prolonged the time course of HM and AL phosphorylation of PKBR1 (Fig. 6 B), as it did in wild-type cells (Fig. 4 A). In addition, we compared the kinetics of PKBR1 phosphorylation

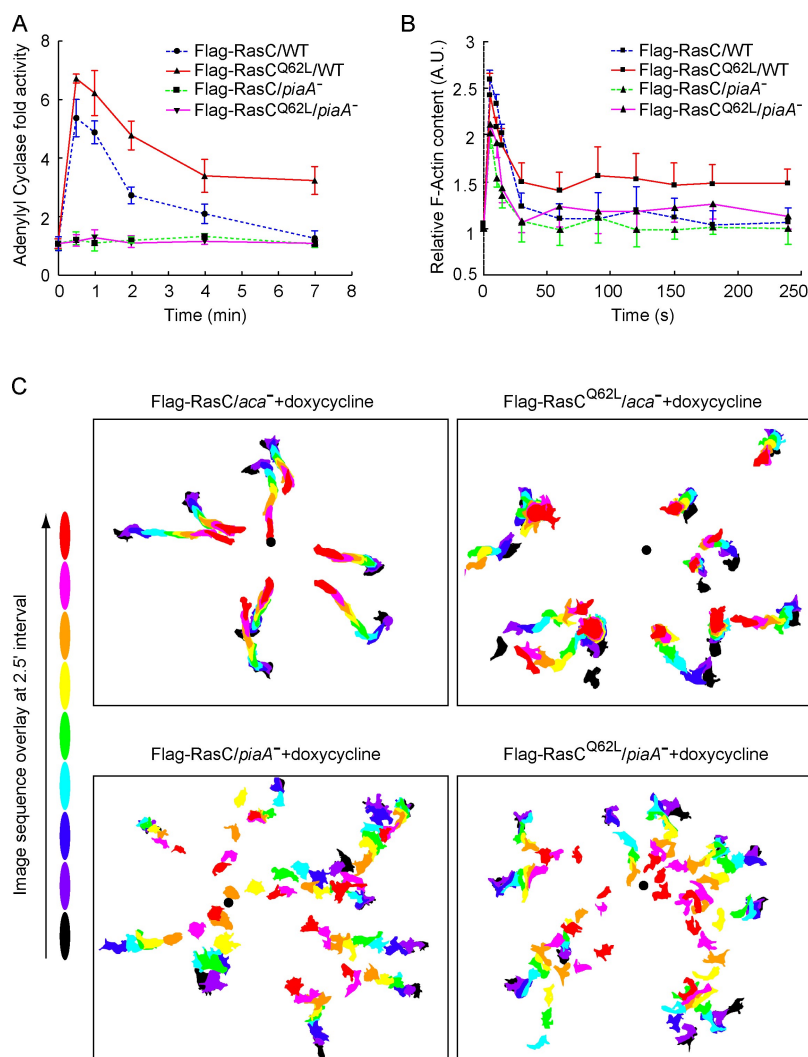


Figure 5. Deletion of PiaA suppresses the unregulated chemotactic responses caused by RasC^{Q62L}. (A and B) ACA activation and actin polymerization were measured in wild-type (WT) or *piaA*[−] cells induced to express Flag-RasC or -RasC^{Q62L}. ACA data represent the range (mean \pm standard error) of two independent experiments. The basal activities ranged from 15.2 pmol/min/mg protein for Flag-RasC/*piaA*[−] and -RasC^{Q62L}/*piaA*[−] cells to 17.9 pmol/min/mg protein for Flag-RasC/WT and 19.2 pmol/min/mg protein for Flag-RasC^{Q62L}/WT cells. For the actin polymerization assay, the data represent mean \pm SD of three independent experiments. A.U., arbitrary unit. (C) The micropipette assay was performed in *aca*[−] or *piaA*[−] cells induced to express Flag-RasC or -RasC^{Q62L}.

in wild-type cells and cells lacking the phosphoinositide 3-phosphatase PTEN (phosphatase and tensin homologue on chromosome 10), in which the chemoattractant-triggered production of PIP3 is greatly extended (Iijima and Devreotes, 2002; Zhang et al., 2008), and found no significant difference (Fig. 6 C). In contrast, AL phosphorylation of PKBA was increased in *pten*[−] cells (Fig. 6 C). Together, these results demonstrate that PIP3 is not required for the prolonged activation of PKBR1 triggered by RasC^{Q62L}.

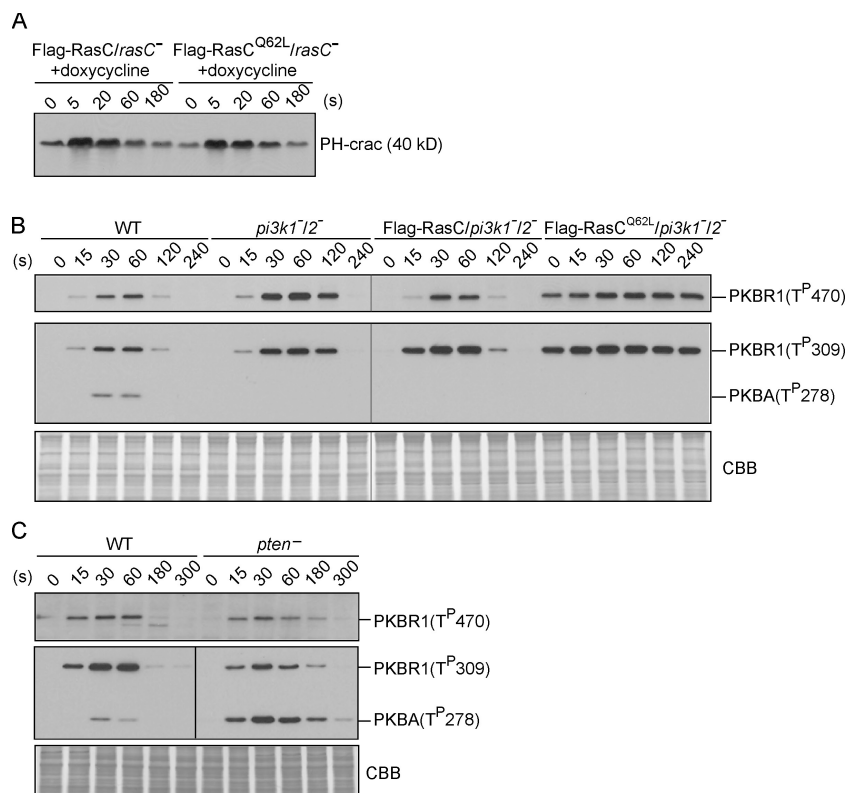
RasC activates TORC2 to phosphorylate PKBR1 in in vitro reconstitution assays

We used a cell-free system to further elucidate the role of RasC in activation of the TORC2–PKB pathway. The HM of PKBR1 and ALs of both PKBR1 and PKBA were rapidly phosphorylated after the application of GTP- γ S to lysates of wild-type cells (Fig. 7 A). The addition of excess GST-tagged RBD but not GST inhibited these GTP- γ S-induced phosphorylation events (Fig. 7 A), suggesting that GTP- γ S functions through Ras proteins to activate TORC2. To test whether RasC specifically activates TORC2, we also examined PKB phosphorylation in unstimulated lysates (with no chemoattractant or GTP- γ S added) from wild-type cells (Fig. 7 B, lane 1), *piaA*[−] cells expressing Flag-RasC^{Q62L}

(Fig. 7 B, lane 2), and their mixture (Fig. 7 B, lane 5). We reasoned that if RasC is responsible for TORC2 activation, RasC^{Q62L} from the Flag-RasC^{Q62L}/*piaA*[−] cell lysates should be able to activate TORC2 from the wild-type cell lysates to phosphorylate the PKBs. Indeed, recapitulation of PKB phosphorylation was only achieved by mixing the two lysates (Fig. 7 C). The reconstitution of PKB phosphorylation could be inhibited by the addition of GST-RBD (Fig. 7 B, lane 7) but not GST (Fig. 7 B, lane 6). Moreover, PKB phosphorylation could not be reconstituted by the combination of Flag-RasC/*piaA*[−] and wild-type cell lysates (Fig. 7, B [lane 3] and C) or Flag-RasC^{Q62L}/*piaA*[−] and *piaA*[−] cell lysates (Fig. 7, B [lane 4] and C). As a control, we also performed the reconstitution assay in the presence of excessive GDP- β S, which would prevent the activation of any other GTPases if present in the system, and found no significant effect (Fig. 7 D). Together, these results indicate that activated RasC is sufficient to trigger PKB phosphorylation via TORC2.

The in vitro system allowed us to further investigate the mechanism of RasC-mediated activation of TORC2. When lysates from wild-type as well as *piaA*[−] cells expressing Flag-PiaA were fractionated, the high-speed supernatant (HSS) fractions were found to be able to reconstitute PKB phosphorylation in the presence of RasC^{Q62L} (Fig. 8 A, lanes 1 and 2). Reconstitution

Figure 6. PIP3 is not required for RasC-mediated activation of the TORC2-PKBR1 pathway. (A) PHc-rac-GFP translocation assay, which measures PIP3 content on the membrane, was performed in *rasC*⁻ cells induced to express Flag-RasC or -RasC^{Q62L}. (B) Phosphorylation of PKB was measured in wild-type (WT), *pi3k1*⁻/*2*⁻, and *pi3k1*⁻/*2*⁻ cells expressing Flag-RasC or -RasC^{Q62L}. The protein-transferred membrane was stained with Coomassie brilliant blue (CBB) and shown as loading control. (C) Phosphorylation of PKB was measured in wild-type and *pten*⁻ cells. The protein-transferred membrane was stained with Coomassie brilliant blue and shown as loading control. (B and C) Vertical black lines indicate that intervening lanes have been spliced out.



could also be achieved with Flag immunoprecipitate from Flag-PiaA/*piaA*⁻ HSS (Fig. 8 A, lane 4) but not Flag/*piaA*⁻ HSS (Fig. 8 A, lane 3). However, the Flag-PiaA immunoprecipitate was not sufficient to phosphorylate the two PKBs when added to lysates from *piaA*⁻ cells expressing Flag-RasC (Fig. 8 A, lane 5). Collectively, these results suggest that the Flag-PiaA immunoprecipitate is likely to contain a TORC2 complex that can be activated by RasC^{Q62L}.

To further substantiate this conclusion, we tested the reconstituting activity of the Flag-PiaA immunoprecipitate against membrane fractions prepared from *piaA*⁻ cells as well as total lysates from *rip3*⁻ cells expressing Flag-RasC or -RasC^{Q62L}, all of which are depleted of intact TORC2 complex. We found that the Flag-PiaA immunoprecipitate was able to specifically reconstitute PKB phosphorylation when mixed with membranes isolated from Flag-RasC^{Q62L}/*piaA*⁻ cells (Fig. 8 B) as well as with lysates from Flag-RasC^{Q62L}/*rip3*⁻ cells (Fig. 8 C), indicating that the Flag-PiaA immunoprecipitate contains a functional TORC2 complex. Consistent with this finding, we found that Flag-PiaA immunoprecipitated from *rip3*⁻ cells lacks the reconstituting activity (Fig. 8 D). Furthermore, we found that the ability of the Flag-PiaA immunocomplex to reconstitute PKB phosphorylation depends on TOR activity because it could be blocked by the TOR-specific ATP-competitive inhibitor PP242 (Feldman et al., 2009) with an IC₅₀ of ~4 nM (Fig. 8 E). Together, these results demonstrate that the RasC-TORC2-PKB pathway can be reconstituted in vitro.

Finally, we performed a coimmunoprecipitation experiment to examine the physical interaction between TORC2 and RasC. To this end, we expressed T7-tagged Rip3 in *rip3*⁻ cells, which restored the defects of PKB phosphorylation in these

cells (unpublished data). We then coexpressed T7-Rip3 with Flag-RasC or -RasC^{Q62L} and performed immunoprecipitation with anti-T7 antibody. As shown in Fig. 8 F, Flag-RasC and -RasC^{Q62L} were expressed at comparable levels. However, only Flag-RasC^{Q62L} was specifically immunoprecipitated with T7-Rip3 (Fig. 8 F), indicating that activated RasC interacts either directly with Rip3 or with another component of the TORC2 complex that links to Rip3. This result shows that RasC and TORC2 interact in a regulated fashion and further supports the conclusion that activated RasC is able to stimulate TORC2 activity.

Discussion

Compared with their widely known function in cell growth, differentiation, and tumorigenesis, the role of Ras proteins in cell motility has been relatively unexplored. In the current work, we performed a series of experiments to investigate how RasC regulates chemotaxis via TORC2. Based on our results, we propose a network of signaling events centered around Ras-mediated activation of TORC2 that controls cytoskeletal activity and chemotaxis. As illustrated in Fig. 9, chemoattractants activate RasC through the G protein-coupled receptor cAR1, leading to TORC2-mediated activation of PKBR1 and PKBA, which phosphorylate PKB substrates and regulate chemotactic responses of the cell. This model is supported by several findings. First, we show that gain of function in RasC results in prolonged phosphorylation of PKBR1 and PKB substrates (Fig. 2), which in turn leads to extended ACA activation, elevated actin polymerization, and impaired chemotaxis (Fig. 3). Second, disruption of TORC2 activity specifically suppresses the aberrant chemotactic responses caused by persistently activated RasC (Figs. 4 and 5). Third,

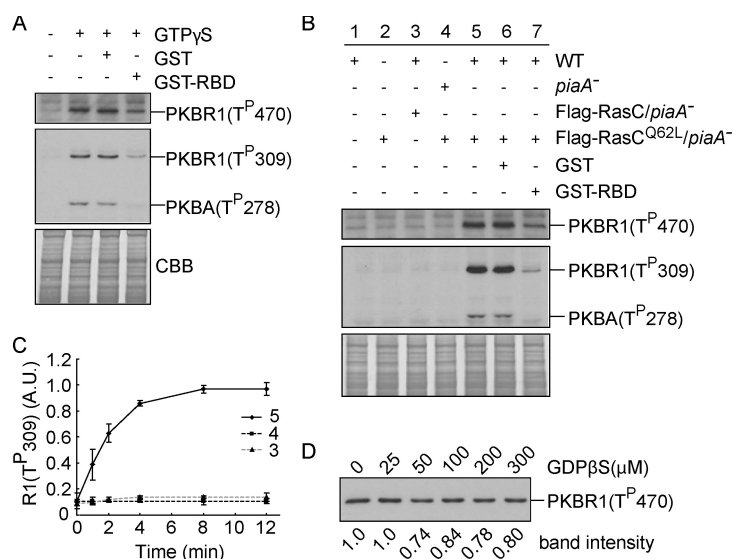


Figure 7. RasC^{Q62L} activates TORC2-mediated phosphorylation of PKB in vitro. (A) Wild-type cell lysates were stimulated with GTP-γS alone or in the presence of GST or GST-RBD and then probed with phospho-specific antibodies. The protein-transferred membrane was stained with Coomassie brilliant blue (CBB) and shown as loading control. (B) The indicated cell lines were mixed, lysed, incubated in the presence or absence of GST or GST-RBD for 12 min, and then probed with phospho-specific antibodies. The protein-transferred membrane was stained with Coomassie brilliant blue and shown as loading control. Cells were not stimulated with chemoattractant, nor was GTP-γS added to the reaction. WT, wild type. (C) Quantitative densitometry of the time courses of reactions 3, 4, and 5 of B. The data represent mean ± SD of three independent experiments. A.U., arbitrary unit. (D) *piaA*⁻ cells expressing Flag-RasC^{Q62L} were mixed with wild-type cells in the presence of increasing concentrations of GDP-βS, filter lysed, incubated on ice for 12 min, and then probed with anti-phospho-HM antibody.

RasC is required for activation of the PKBs in vivo (Fig. 1) and stimulates TORC2-dependent phosphorylation of the PKBs in vitro (Figs. 7 and 8). Fourth, we show that RasC does not activate PI3Ks and that the activation of the TORC2 pathway by RasC does not require PIP3 (Fig. 6). We conclude that there is a RasC–TORC2–PKB pathway in *D. discoideum* that plays a major role in temporal and spatial regulation of chemotactic responses. This finding has several implications in our understanding of chemotaxis and TORC2 signaling.

Our results provide new insights about the negative regulators in the chemotactic signaling pathways. Many G protein-coupled signaling events rapidly subside when cells are exposed to a step increase in chemoattractant. The time courses of RasC activation, PKB phosphorylation, and downstream chemotactic responses all reflect this rapid shutoff (Figs. 2 and 3). When the activation of RasC is prolonged, as in cells expressing the Q62L or G13V mutation, the kinetics of all of the downstream responses are similarly extended, suggesting that RasC inactivation is a rate-limiting step for the shutoff. Previous experiments of G protein signaling showed that α and βγ subunits of G protein remain dissociated (i.e., activated) as long as chemoattractant receptors are occupied (Janetopoulos et al., 2001). Together, these results argue that the site of shutoff lies between G proteins and the Ras regulators (Fig. 9).

Why does prolonged activation of RasC impair chemotaxis? Chemotaxis involves the interaction between spontaneous motility and directional sensing. In the absence of a chemoattractant gradient, actin-based membrane protrusions are formed along the cell perimeter, propelling the cell in random directions. In a gradient, directional sensing generates intracellular asymmetries that bias motility. Activation of Ras proteins and TORC2-mediated PKB phosphorylation have been shown to occur selectively at the leading edge of chemotaxing cells as well as at the tips of pseudopodia and are thus in a position to bias motility (Sasaki et al., 2004, 2007; Kamimura et al., 2008). We speculate that extending RasC activation interferes with chemotaxis in multiple ways. First, pseudopodia extension and retraction that underlie random migration as well as chemotaxis likely

depend on the timely activation and inactivation of Ras proteins. Indeed, we have observed that both basal motility and responses to chemotactic stimuli are altered in cells expressing RasC^{Q62L}. The character and distribution of pseudopods in cells expressing RasC^{Q62L} appear to be different from those in wild-type cells (Fig. 3). Second, because the dispersion length of a protein is proportional to its half-life, the constitutively activated form of RasC^{Q62L} is expected to have a broader spatial distribution than that of wild-type RasC. As RasC^{Q62L} diffuses further before being inactivated, the downstream responses it controls will be delocalized as well, impairing cells' ability to interpret the directional signal. Therefore, the rapid inactivation of RasC is critical for localizing downstream responses and directional sensing.

Our results provide the first substantial evidence that TORC2 is under the control of a Ras protein and open the possibility for further study of the regulatory mechanism of TORC2. Loss of function in RasC greatly reduces PKB phosphorylation (Fig. 1), and the effects of RasC^{Q62L} on PKBR1 phosphorylation are suppressed by deleting *PiaA* (Fig. 4). These in vivo results indicate that the major effects of RasC on chemotaxis are mediated through TORC2 and PKBR1. The active form of RasC promotes TORC2-dependent phosphorylation of the two PKBs in vitro in the absence of any stimulus (Figs. 7 and 8). This reaction exhibits several characteristics that are consistent with a RasC–TORC2–PKB pathway. It is blocked by exogenous RBD and does not occur in lysates lacking the TORC2 component *PiaA* or *Rip3* but can be rapidly initiated by adding Flag immunoprecipitate from *piaA*⁻ cells expressing Flag-*PiaA*. Further experiments indicate that the reconstituting activity associated with the Flag immunoprecipitate likely contains a functional TOR complex (Fig. 8, B–D). Importantly, TORC2 binds specifically to RasC^{Q62L} but not to inactivated wild-type RasC (Fig. 8 F), suggesting that a regulated interaction may contribute to the stimulation of TORC2 activity by RasC^{Q62L}. Interestingly, we found that RasC^{Q62L} lacking the C-terminal CAAX motif is not able to extend the kinetics of PKB phosphorylation (unpublished data), indicating that the membrane localization of RasC is critical for its in vivo function in activating TORC2.

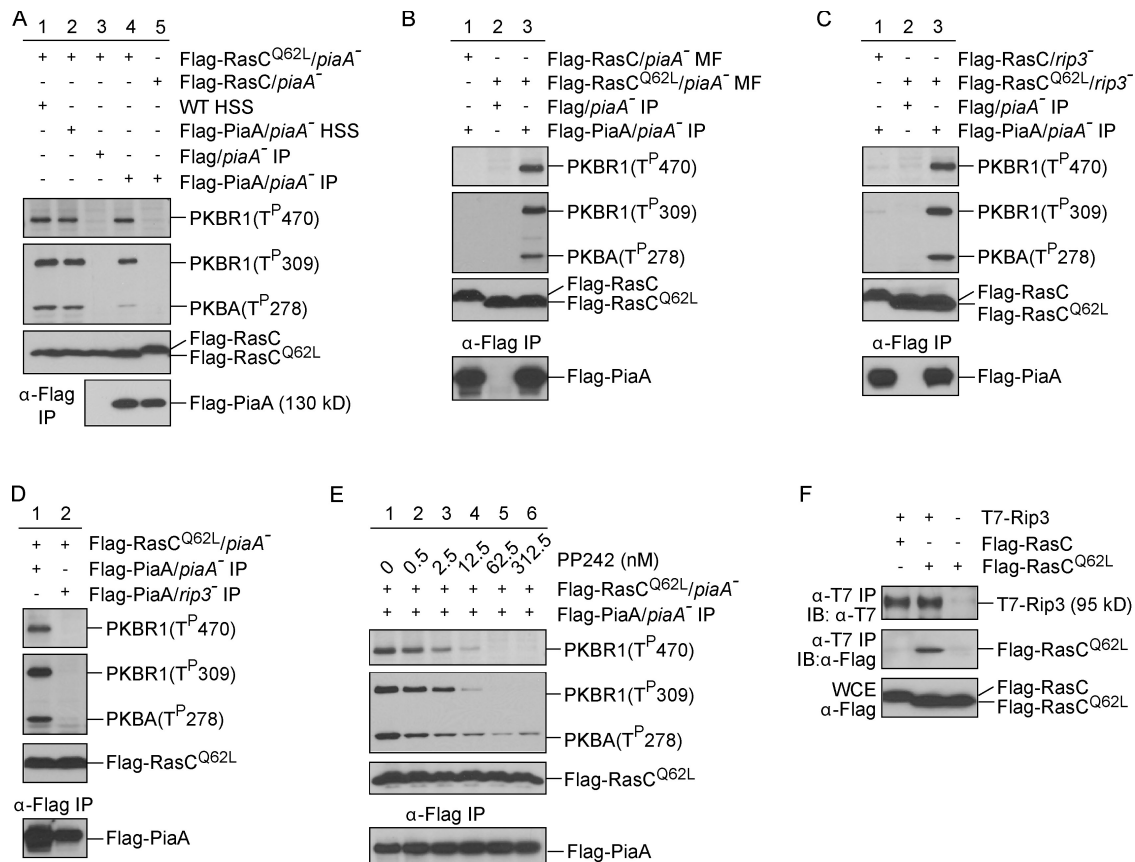


Figure 8. Reconstitution of PKB activation in vitro with immunopurified TORC2. (A) Cell lysates from *piaA*⁻ cells expressing Flag-RasC or -RasC^{Q62L} were mixed with HSS made from wild-type (WT) cells or *piaA*⁻ cells expressing Flag-PiaA or with Flag-eluted immunoprecipitate from Flag/*piaA*⁻ cells or Flag-PiaA/*piaA*⁻ cells. (B) Membrane fractions (MF) prepared from Flag-RasC/*piaA*⁻ or Flag-RasC^{Q62L}/*piaA*⁻ cells were mixed with Flag-eluted immunoprecipitate from Flag/*piaA*⁻ cells or Flag-PiaA/*piaA*⁻ cells. (C) Cell lysates from *rip3*⁻ cells expressing Flag-RasC or -RasC^{Q62L} were mixed with Flag-eluted immunoprecipitate from Flag/*piaA*⁻ cells or Flag-PiaA/*piaA*⁻ cells. (D) Cell lysates from *piaA*⁻ cells expressing Flag-RasC^{Q62L} were mixed with Flag-eluted immunoprecipitate from Flag-PiaA/*piaA*⁻ cells or Flag-PiaA/*rip3*⁻ cells. (E) Flag-eluted immunoprecipitate from Flag-PiaA/*piaA*⁻ cells was treated with increasing concentrations of PP242 before being mixed with cell lysates from *piaA*⁻ cells expressing Flag-RasC^{Q62L}. (F) Whole cell extracts were prepared from *rip3*⁻ cells expressing T7-Rip3 and Flag-RasC, T7-Rip3 and Flag-RasC^{Q62L}, or Flag-RasC^{Q62L} alone. Immunoprecipitation (IP) was performed using anti-T7 antibody, and samples were immunoblotted (IB) with anti-T7 or anti-Flag antibodies.

A role for a Ras protein in PKB activation and cell migration may not seem surprising, as it has been shown that Ras proteins bind to both *D. discoideum* and mammalian PI3Ks (Rodriguez-Viciano et al., 1994; Pacold et al., 2000; Funamoto et al., 2002; Kae et al., 2004). However, our data show that the effects of RasC^{Q62L} on chemotactic responses and the cytoskeletal activity are primarily mediated through TORC2. Furthermore, we found that disruption of PKBA but not PKBR1 in *pten*⁻ cells suppresses its chemotaxis defects (unpublished data). Therefore, although expressing RasC^{Q62L} and deleting PTEN both result in hyperstimulation of the PKB signaling, their effects appear to be mediated through different PKB isoforms. Our finding that TORC2 is a critical effector in Ras-mediated cell migration may serve as a stepping stone to understand cell motility in other organisms. PIP3-independent chemotaxis and chemoattractant-stimulated Ras activation have also been observed in human neutrophils (Worthen et al., 1994; Zheng et al., 1997). In many cancer cells that display altered cell migration, Ras proteins are found to be persistently activated (Oxford and Theodorescu, 2003). In addition, TORC2 has been suggested to regulate cytoskeletal-based events in various systems (Jacinto et al., 2004;

Sarbasov et al., 2004; Kamada et al., 2005). It will be of great interest to learn whether the Ras–TORC2 pathway plays a similar role in the cytoskeleton organization and migration of these cells.

Materials and methods

Cell growth and differentiation

Cells were cultured axenically in HL5 medium at 22°C. Cells carrying expression constructs were maintained in HL5 medium containing 10–20 µg/ml G418 or 30–40 µg/ml hygromycin, or both as required. For differentiation, cells grown in HL5 were washed with development buffer (DB; 5 mM Na₂HPO₄, 5 mM KH₂PO₄, 2 mM MgSO₄, and 0.2 mM CaCl₂), starved in DB for 1 h at 2 × 10⁷ cells/ml, and then pulsed with 50 nM cAMP every 6 min for 4.5 h. To induce the expression of Flag-RasC or -RasC^{Q62L}, doxycycline was added during the last 2 h of differentiation at a concentration of 40 µg/ml.

Gene disruption and plasmid construction

rasC⁻ cells were constructed in an AX2 background. A disruption cassette, consisting of a genomic DNA fragment amplified by PCR using primers 5'-CATTGCGATTGATAATACACAATAAATCA-3' and 5'-GGGGTTGGATCAT-ATTCAGCAATGAATTGA-3', the Blasticidin S resistant (BSR) cassette from pLPBP (Faix et al., 2004), followed by a genomic DNA fragment amplified by PCR using primers 5'-GAGCAAGGATGTTCTAATTGAATTGATTTC-3' and 5'-GGGCATCAGCCAAATCTAGAGTAAACGTT-3', was used to target the

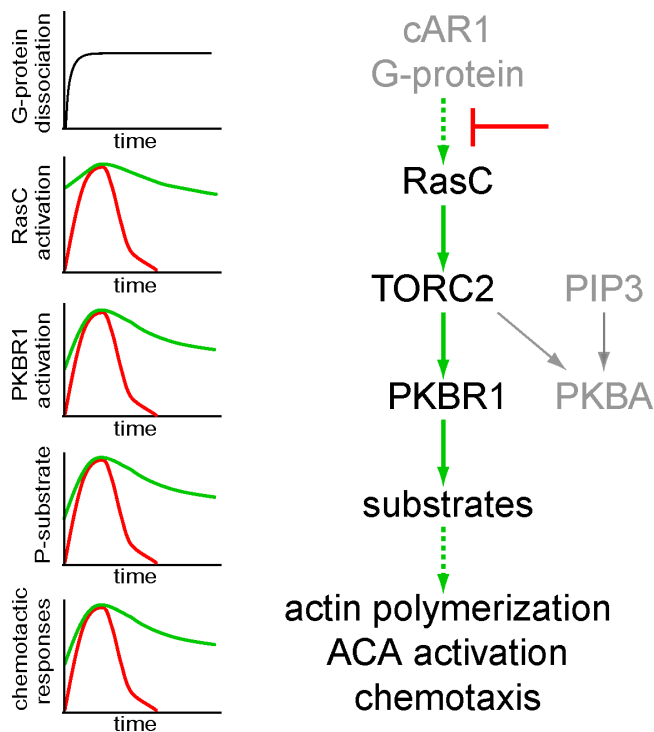


Figure 9. Schematic diagram of RasC-mediated signaling pathways that control chemotaxis. The chemoattractant cAMP signals through the G protein-coupled receptor cAR1 to RasC, leading to TORC2-mediated activation of PKBR1 and PKBA. The activation of PKBA also depends on recruitment to PIP3. Together, the two PKBs phosphorylate a series of substrates and play a critical role in ACA activation, actin polymerization, and chemotaxis. The graphs to the left schematically illustrate the kinetics of G protein α and $\beta\gamma$ subunits dissociation, RasC activation, PKB phosphorylation, PKB substrate phosphorylation, and chemotactic responses. The red line shows the typical wild-type responses that are rapidly shut off during persistent stimulation. The green line shows the responses in cells in which the inhibitory signal indicated by (–) is bypassed by RasC^{Q62L}.

gene for deletion by homologous recombination. Knockouts were screened by PCR and confirmed by Southern blotting. Flag-RasC was amplified by PCR using primers 5'-AAATAAAATGGATTATAAAGATGATGATGATAATCAAAATTATATAAATTAG-3' and 5'-TTACAATATAATACATCCCT-3' from *rasC* cDNA plasmid. The resulting PCR fragment was cloned into the BglIII site of pDM359 (Veltman et al., 2009) for doxycycline-inducible expression or the BglIII site of pJ1 for constitutive expression. To create activated RasC, the conserved glycine at position 13 or glutamine at position 62 was mutated to valine or leucine, respectively, by quick change site-directed mutagenesis.

Immunoblotting

Differentiated cells were shaken at 200 rpm in DB with 5 mM caffeine for 20 min, washed with PM buffer (5 mM Na₂HPO₄, 5 mM KH₂PO₄, and 2 mM MgSO₄) twice, resuspended to 2×10^7 cells/ml in PM, and kept on ice before assay. Cells were stimulated with 1 μ M cAMP, lysed in SDS sample buffer at various time points, and boiled for 5 min. Immunoblotting was performed as described previously (Kamimura et al., 2009). Antibodies recognizing specific phosphorylated sites were purchased from Cell Signaling Technology. Anti-phospho-PKB substrate antibody (rabbit monoclonal antibody) was used to detect the phosphorylation of the substrates of PKBA and PKBR1. Anti-phospho-PDK docking motif antibody (mouse monoclonal antibody) was used to detect the phosphorylation of the HM of PKBR1. Anti-phospho-PKC (pan) antibody (rabbit monoclonal antibody) was used to detect the phosphorylation of the ALs of both PKBA and PKBR1. Monoclonal antibody from Sigma-Aldrich was used to detect the Flag tag. Anti-pan-Ras mouse monoclonal antibody from EMD was used to detect *D. discoideum* Ras proteins. Anti-T7 tag monoclonal antibody from EMD was used to detect the T7 tag.

In vitro PKB phosphorylation assay

For GTP- γ S-stimulated PKB phosphorylation, cells were pretreated with caffeine as described in the previous section, resuspended in PM at a density of

8×10^7 cells/ml, and kept on ice before assay. 100 μ l of cell suspension was mixed with equal volume of TM buffer (20 mM Tris, pH 8.0, and 2 mM MgSO₄) in the presence or absence of 40 μ M GTP- γ S (Roche) and then immediately lysed through two layers of 5- μ m filter membranes. Lysate samples were incubated on ice for 8–12 min before being stopped by the addition of SDS sample buffer. To test whether Ras proteins mediate the effects of GTP- γ S, 10 μ g GST-RBD or an equal amount of GST purified from bacteria was added together with GTP- γ S.

To reconstitute PKB phosphorylation in vitro with lysates from wild-type cells and *piaA*[–] cells expressing Flag-RasC^{Q62L}, 50 μ l of cell suspension from each cell line was mixed together with 100 μ l TM and 1 μ l of 60 mM ATP and then filter lysed. Reactions were incubated on ice for 8–12 min and stopped by the addition of SDS sample buffer.

To make HSS, caffeine-treated cells were washed with PM twice, resuspended in glycerol lysis buffer (20 mM Tris, pH 8.0, 2 mM MgSO₄, 0.2 mM EGTA, 10% glycerol, and complete EDTA-free protease inhibitor [Roche]) at a density of 8×10^7 cells/ml, and filter lysed. Cell lysates were centrifuged at 53,000 rpm in a TLA55 rotor (Beckman Coulter) at 4°C for 1 h, and the supernatant was collected. 100 μ l of the supernatant was used in one reaction.

To prepare membrane fractions from *piaA*[–] cells expressing Flag-RasC or Flag-RasC^{Q62L}, differentiated cells were resuspended in PM at a density of 8×10^7 cells/ml and filter lysed. Cell extracts were centrifuged at 16,000 g for 2 min. The membrane pellet was washed once with PM, resuspended with 100 μ l PM, and used in one reaction.

To obtain Flag-PiaA immunocomplex used for experiments presented in Fig. 8 (B–E), Flag-PiaA was immunoprecipitated as follows: 20 μ l anti-Flag M2 affinity gel (Sigma-Aldrich) was incubated with 1.2 ml HSS at 4°C for 3 h, washed with glycerol lysis buffer for three times and a total of 15 min, and then eluted with 100 μ l of 500 ng/ μ l 3xFlag peptide (Sigma-Aldrich) at 4°C for 30 min. 100 μ l of the eluate was used in one reaction. For experiments illustrated in Fig. 8 A, 200 ng/ μ l 3xFlag peptide was used to elute the complex. For PP242 treatment, the Flag-PiaA eluate was incubated with PP242 for 15 min on ice before 0.1 mM ATP and lysates from Flag-RasC^{Q62L}/*piaA*[–] cells were added. The reaction was continued on ice for another 12 min before being stopped by the addition of SDS sample buffer.

Coimmunoprecipitation assay

rip3[–] cell was cotransformed with constructs expressing T7-Rip3 and Flag-RasC, or T7-Rip3 and Flag-RasC^{Q62L}, or Flag-RasC^{Q62L} only. Cells were differentiated, washed twice with PM, and lysed with immunoprecipitation buffer (20 mM Tris, pH 8.0, 20 mM MgCl₂, 0.2 mM EGTA, 10% glycerol, complete EDTA-free protease inhibitor, 2 mM Na₂VO₄, and 0.3% CHAPS) for 10 min on ice. Cell extracts were centrifuged at 16,000 g for 2 min. Supernatant fraction was collected and incubated with 3 μ l anti-T7 antibody at 4°C for 3 h. The immunocomplex was recovered by protein G-Sepharose beads (GE Healthcare) during a 1-h incubation at 4°C. Beads were washed four times with immunoprecipitation buffer, and proteins were eluted by boiling the beads in SDS sample buffer.

Micropipette assay and image acquisition

Differentiated cells were plated on coverslip chambers (NalgenNunc; LabTek) filled with DB and allowed to adhere to the surface for ~15–20 min. A micropipette filled with 1 μ M cAMP was placed into the field of view. Chemotaxis was recorded by time-lapse video using an inverted microscope (CKX41; Olympus) with a 20 \times NA 0.4 objective lens. Images were captured with ImageJ software (National Institutes of Health). Motility speed was calculated as the total distance traveled by the cell divided by time. To calculate chemotactic index, the cosine of the angle between the direction of movement and the direction of chemoattractant gradient was determined for each frame. The values were weighted according to the length of the step and averaged. The distances between the start (d1) and the end (d2) point of the migration path to the needle were measured, and chemotactic motility was calculated as (d1 – d2) divided by the time the cell travels from the start to the end point. Persistency was calculated as the shortest linear distance between the start point and end point of the migration path divided by the total distance traveled by the cell.

1 μ M cAMP was used to stimulate the translocation of LimE Δ coi-RFP. Cells were observed with a spinning disk confocal microscope (UltraVIEW DM16000; PerkinElmer) using a 40 \times NA 1.25-0.75 oil immersion objective. Images were captured with a cooled 12-bit charge-coupled device camera (LSI) and the Slidebook 4.0 software (Intelligent Imaging Innovations, Inc.) and processed using Photoshop 7.0 and Illustrator 10.0 (Adobe). All experiments were performed at RT.

PH domain translocation assay

The assay was performed as described previously (Lilly and Devreotes, 1995). In brief, differentiated cells were treated with caffeine and resuspended in PM at a density of 8×10^7 cells/ml. At specific time points after stimulation with 1 μ M cAMP, 100- μ l aliquots of cells were filter lysed. Cell lysates were immediately mixed with equal volumes of supernatant containing PHcrac-GFP. Reactions were incubated on ice for 30 s before being stopped by the addition of 1 ml ice-cold PM. Membrane fractions were collected and blotted with anti-GFP antibody.

Actin polymerization assay

Cells were pretreated with 3 mM caffeine for 20 min, washed with PM, resuspended in PM plus 1 mM caffeine at a density of 2×10^7 cells/ml, and kept on ice before assay. Cells were warmed by shaking at RT for 10 min and then stimulated with 1 μ M cAMP. At specific time points after stimulation, aliquots of cells were lysed by the addition of equal volumes of cold 2 \times assay buffer (2% Triton X-100, 20 mM KCl, 20 mM EGTA, 20 mM imidazole, and 0.1 mg/ml Na₂S₂O₃). Cell lysates were incubated at RT for 10 min with occasional agitation. The Triton-insoluble cytoskeletal fraction was collected by centrifugation at 8,000 g for 4 min, washed once with 1 \times assay buffer, dissolved in 2 \times SDS sample buffer, and subjected to SDS-PAGE. The amount of actin was determined by densitometric analysis of scanned Coomassie-stained gels.

ACA assay

Cells were grown to $\sim 5 \times 10^6$ cells/ml in HL5 medium and were allowed to differentiate to the chemotaxis competent stage by resuspending them in DB and providing exogenous pulses of 75 nM cAMP for 5.5 h. The cAMP receptor-mediated activation of ACA was performed as previously described (Kriebel and Parent, 2009). In brief, differentiated cells were treated with 2 mM caffeine for 30 min, washed and resuspended in ice-cold PM buffer, and stimulated with 10 μ M cAMP at RT, except that the basal activity was measured on ice. Cells were withdrawn at the indicated time points into the reaction mix containing α -[³²P]ATP diluted with unlabeled ATP to a final concentration of 100 nM. The reaction was allowed to proceed for 1 min and stopped with SDS/ATP, and the [³²P]cAMP was purified by sequential Dowex AG 50W X-4 and alumina column chromatography.

Online supplemental material

Fig. S1 shows that RasC but not RasG is required for the activation of the PKB pathway. Fig. S2 shows that constitutive expression of activated forms of RasC in *rasC*⁺ cells results in prolonged activation of PKBR1 and defects in chemotaxis. Fig. S3 shows that PKBR1 and PKBA are required for ACA activation. Fig. S4 shows that RasC is activated in *piaA*⁺ cells. Videos 1 and 2 show the translocation of LimE Δ coil-RFP in *rasC*⁺ *D. discoideum* cells induced to express Flag-RasC or -RasC^{Q62L}. Videos 3–10 show different lines of *D. discoideum* cells migrating in a gradient of cAMP generated by a micropipette. Online supplemental material is available at <http://www.jcb.org/cgi/content/full/jcb.201001129/DC1>.

We thank Y. Xiong from Dr. P.A. Iglesias' laboratory for help with chemotaxis video analysis, Dr. P. Van Haastert for providing the doxycycline-inducible expression vector, Dr. G. Weeks for the GST-RBD construct and RasC antibody, Dr. R.A. Firtel for the T7-Rip3 construct, Dr. R. Insall for the *rasG*⁺ cell, M. Tang from the Devreotes laboratory for the *piaA*⁺ cell, the *D. discoideum* cDNA project, and National BioResource Project for providing the RasC cDNA, and the proteomics core facility in Johns Hopkins University, School of Medicine, for mass spectrometry analysis.

This work was supported by National Institutes of Health (NIH) grants GM 28007 and GM 34933 to P.N. Devreotes and by the Intramural Research Program of the NIH, National Cancer Institute, Center for Cancer Research. H. Cai is a recipient of Helen Hay Whitney postdoctoral fellowship.

Submitted: 25 January 2010

Accepted: 29 June 2010

References

Cantley, L.C. 2002. The phosphoinositide 3-kinase pathway. *Science*. 296:1655–1657. doi:10.1126/science.296.5573.1655

Chen, M.Y., Y. Long, and P.N. Devreotes. 1997. A novel cytosolic regulator, Pianissimo, is required for chemoattractant receptor and G protein-mediated activation of the 12 transmembrane domain adenylyl cyclase in *Dictyostelium*. *Genes Dev*. 11:3218–3231. doi:10.1101/gad.11.23.3218

Faix, J., L. Kreppel, G. Shaulsky, M. Schleicher, and A.R. Kimmel. 2004. A rapid and efficient method to generate multiple gene disruptions in *Dictyostelium discoideum* using a single selectable marker and the Cre-loxP system. *Nucleic Acids Res*. 32:e143. doi:10.1093/nar/ghn136

Feig, L.A., and G.M. Cooper. 1988. Relationship among guanine nucleotide exchange, GTP hydrolysis, and transforming potential of mutated ras proteins. *Mol. Cell. Biol*. 8:2472–2478.

Feldman, M.E., B. Apse, A. Uotila, R. Loewith, Z.A. Knight, D. Ruggero, and K.M. Shokat. 2009. Active-site inhibitors of mTOR target rapamycin-resistant outputs of mTORC1 and mTORC2. *PLoS Biol*. 7:e38. doi:10.1371/journal.pbio.1000038

Franca-Koh, J., Y. Kamimura, and P. Devreotes. 2006. Navigating signaling networks: chemotaxis in *Dictyostelium discoideum*. *Curr. Opin. Genet. Dev*. 16:333–338. doi:10.1016/j.gde.2006.06.001

Frias, M.A., C.C. Thoreen, J.D. Jaffe, W. Schroder, T. Sculley, S.A. Carr, and D.M. Sabatini. 2006. mSin1 is necessary for Akt/PKB phosphorylation, and its isoforms define three distinct mTORC2s. *Curr. Biol*. 16:1865–1870. doi:10.1016/j.cub.2006.08.001

Funamoto, S., R. Meili, S. Lee, L. Parry, and R.A. Firtel. 2002. Spatial and temporal regulation of 3-phosphoinositides by PI 3-kinase and PTEN mediates chemotaxis. *Cell*. 109:611–623. doi:10.1016/S0092-8674(02)00755-9

Huang, Y.E., M. Iijima, C.A. Parent, S. Funamoto, R.A. Firtel, and P. Devreotes. 2003. Receptor-mediated regulation of PI3Ks confines PI(3,4,5)P₃ to the leading edge of chemotaxing cells. *Mol. Biol. Cell*. 14:1913–1922. doi:10.1091/mbc.E02-10-0703

Huang, J., C.C. Dibble, M. Matsuzaki, and B.D. Manning. 2008. The TSC1-TSC2 complex is required for proper activation of mTOR complex 2. *Mol. Cell. Biol*. 28:4104–4115. doi:10.1128/MCB.00289-08

Iglesias, P.A., and P.N. Devreotes. 2008. Navigating through models of chemotaxis. *Curr. Opin. Cell Biol*. 20:35–40. doi:10.1016/j.ccb.2007.11.011

Iijima, M., and P. Devreotes. 2002. Tumor suppressor PTEN mediates sensing of chemoattractant gradients. *Cell*. 109:599–610. doi:10.1016/S0092-8674(02)00745-6

Jacinto, E., R. Loewith, A. Schmidt, S. Lin, M.A. Ruegg, A. Hall, and M.N. Hall. 2004. Mammalian TOR complex 2 controls the actin cytoskeleton and is rapamycin insensitive. *Nat. Cell Biol*. 6:1122–1128. doi:10.1038/ncb1183

Janetopoulos, C., T. Jin, and P. Devreotes. 2001. Receptor-mediated activation of heterotrimeric G-proteins in living cells. *Science*. 291:2408–2411. doi:10.1126/science.1055835

Kae, H., C.J. Lim, G.B. Spiegelman, and G. Weeks. 2004. Chemoattractant-induced Ras activation during *Dictyostelium* aggregation. *EMBO Rep*. 5:602–606. doi:10.1038/sj.embor.7400151

Kamada, Y., Y. Fujioka, N.N. Suzuki, F. Inagaki, S. Wullschlegel, R. Loewith, M.N. Hall, and Y. Ohsumi. 2005. Tor2 directly phosphorylates the AGC kinase Ypk2 to regulate actin polarization. *Mol. Cell. Biol*. 25:7239–7248. doi:10.1128/MCB.25.16.7239-7248.2005

Kamimura, Y., and P.N. Devreotes. 2010. Phosphoinositide-dependent protein kinase (PDK) activity regulates phosphatidylinositol 3,4,5-trisphosphate-dependent and -independent protein kinase B activation and chemotaxis. *J. Biol. Chem*. 285:7938–7946. doi:10.1074/jbc.M109.089235

Kamimura, Y., Y. Xiong, P.A. Iglesias, O. Hoeller, P. Bolourani, and P.N. Devreotes. 2008. PIP3-independent activation of TorC2 and PKB at the cell's leading edge mediates chemotaxis. *Curr. Biol*. 18:1034–1043. doi:10.1016/j.cub.2008.06.068

Kamimura, Y., M. Tang, and P. Devreotes. 2009. Assays for chemotaxis and chemoattractant-stimulated TorC2 activation and PKB substrate phosphorylation in *Dictyostelium*. *Methods Mol. Biol*. 571:255–270. doi:10.1007/978-1-60761-198-1_17

Karnoub, A.E., and R.A. Weinberg. 2008. Ras oncogenes: split personalities. *Nat. Rev. Mol. Cell Biol*. 9:517–531. doi:10.1038/nrm2438

King, J.S., and R.H. Insall. 2009. Chemotaxis: finding the way forward with *Dictyostelium*. *Trends Cell Biol*. 19:523–530. doi:10.1016/j.tcb.2009.07.004

Kriebel, P.W., and C.A. Parent. 2009. Group migration and signal relay in *Dictyostelium*. *Methods Mol. Biol*. 571:111–124. doi:10.1007/978-1-60761-198-1_7

Kriebel, P.W., V.A. Barr, and C.A. Parent. 2003. Adenylyl cyclase localization regulates streaming during chemotaxis. *Cell*. 112:549–560. doi:10.1016/S0092-8674(03)00081-3

Lee, S., C.A. Parent, R. Insall, and R.A. Firtel. 1999. A novel Ras-interacting protein required for chemotaxis and cyclic adenosine monophosphate signal relay in *Dictyostelium*. *Mol. Biol. Cell*. 10:2829–2845.

Lee, S., F.I. Comer, A. Sasaki, I.X. McLeod, Y. Duong, K. Okumura, J.R. Yates III, C.A. Parent, and R.A. Firtel. 2005. TOR complex 2 integrates cell movement during chemotaxis and signal relay in *Dictyostelium*. *Mol. Biol. Cell*. 16:4572–4583. doi:10.1091/mbc.E05-04-0342

- Lilly, P.J., and P.N. Devreotes. 1995. Chemoattractant and GTP gamma S-mediated stimulation of adenylyl cyclase in *Dictyostelium* requires translocation of CRAC to membranes. *J. Cell Biol.* 129:1659–1665. doi:10.1083/jcb.129.6.1659
- Lim, C.J., G.B. Spiegelman, and G. Weeks. 2001. RasC is required for optimal activation of adenylyl cyclase and Akt/PKB during aggregation. *EMBO J.* 20:4490–4499. doi:10.1093/emboj/20.16.4490
- Meili, R., C. Ellsworth, S. Lee, T.B. Reddy, H. Ma, and R.A. Firtel. 1999. Chemoattractant-mediated transient activation and membrane localization of Akt/PKB is required for efficient chemotaxis to cAMP in *Dictyostelium*. *EMBO J.* 18:2092–2105. doi:10.1093/emboj/18.8.2092
- Meili, R., C. Ellsworth, and R.A. Firtel. 2000. A novel Akt/PKB-related kinase is essential for morphogenesis in *Dictyostelium*. *Curr. Biol.* 10:708–717. doi:10.1016/S0960-9822(00)00536-4
- Oxford, G., and D. Theodorescu. 2003. Ras superfamily monomeric G proteins in carcinoma cell motility. *Cancer Lett.* 189:117–128. doi:10.1016/S0304-3835(02)00510-4
- Pacold, M.E., S. Suire, O. Perisic, S. Lara-Gonzalez, C.T. Davis, E.H. Walker, P.T. Hawkins, L. Stephens, J.F. Eccleston, and R.L. Williams. 2000. Crystal structure and functional analysis of Ras binding to its effector phosphoinositide 3-kinase gamma. *Cell.* 103:931–943. doi:10.1016/S0092-8674(00)00196-3
- Parent, C.A., B.J. Blacklock, W.M. Froehlich, D.B. Murphy, and P.N. Devreotes. 1998. G protein signaling events are activated at the leading edge of chemotactic cells. *Cell.* 95:81–91. doi:10.1016/S0092-8674(00)81784-5
- Rodriguez-Viciana, P., P.H. Warne, R. Dhand, B. Vanhaesebroeck, I. Gout, M.J. Fry, M.D. Waterfield, and J. Downward. 1994. Phosphatidylinositol-3-OH kinase as a direct target of Ras. *Nature.* 370:527–532. doi:10.1038/370527a0
- Sarbassov, D.D., S.M. Ali, D.H. Kim, D.A. Guertin, R.R. Latek, H. Erdjument-Bromage, P. Tempst, and D.M. Sabatini. 2004. Rictor, a novel binding partner of mTOR, defines a rapamycin-insensitive and raptor-independent pathway that regulates the cytoskeleton. *Curr. Biol.* 14:1296–1302. doi:10.1016/j.cub.2004.06.054
- Sarbassov, D.D., D.A. Guertin, S.M. Ali, and D.M. Sabatini. 2005. Phosphorylation and regulation of Akt/PKB by the rictor-mTOR complex. *Science.* 307:1098–1101. doi:10.1126/science.1106148
- Sasaki, A.T., C. Chun, K. Takeda, and R.A. Firtel. 2004. Localized Ras signaling at the leading edge regulates PI3K, cell polarity, and directional cell movement. *J. Cell Biol.* 167:505–518. doi:10.1083/jcb.200406177
- Sasaki, A.T., C. Janetopoulos, S. Lee, P.G. Charest, K. Takeda, L.W. Sundheimer, R. Meili, P.N. Devreotes, and R.A. Firtel. 2007. G protein-independent Ras/PI3K/F-actin circuit regulates basic cell motility. *J. Cell Biol.* 178:185–191. doi:10.1083/jcb.200611138
- Schneider, N., I. Weber, J. Faix, J. Prassler, A. Müller-Taubenberger, J. Köhler, E. Burghardt, G. Gerisch, and G. Marriotti. 2003. A Lim protein involved in the progression of cytokinesis and regulation of the mitotic spindle. *Cell Motil. Cytoskeleton.* 56:130–139. doi:10.1002/cm.10139
- Veltman, D.M., I. Keizer-Gunnink, and P.J. Haastert. 2009. An extrachromosomal, inducible expression system for *Dictyostelium discoideum*. *Plasmid.* 61:119–125. doi:10.1016/j.plasmid.2008.11.002
- Worthen, G.S., N. Avdi, A.M. Buhl, N. Suzuki, and G.L. Johnson. 1994. FMLP activates Ras and Raf in human neutrophils. Potential role in activation of MAP kinase. *J. Clin. Invest.* 94:815–823. doi:10.1172/JCI117401
- Xiao, Z., N. Zhang, D.B. Murphy, and P.N. Devreotes. 1997. Dynamic distribution of chemoattractant receptors in living cells during chemotaxis and persistent stimulation. *J. Cell Biol.* 139:365–374. doi:10.1083/jcb.139.2.365
- Zhang, S., P.G. Charest, and R.A. Firtel. 2008. Spatiotemporal regulation of Ras activity provides directional sensing. *Curr. Biol.* 18:1587–1593. doi:10.1016/j.cub.2008.08.069
- Zheng, L., J. Eckerdal, I. Dimitrijevic, and T. Andersson. 1997. Chemotactic peptide-induced activation of Ras in human neutrophils is associated with inhibition of p120-GAP activity. *J. Biol. Chem.* 272:23448–23454. doi:10.1074/jbc.272.37.23448